Analytica Chimica Acta: X 4 (2020) 100039

Contents lists available at ScienceDirect

Analytica Chimica Acta: X

journal homepage: www.journals.elsevier.com/analytica-chimica-acta-x

New planar assay for streamlined detection and quantification of β-glucuronidase inhibitors applied to botanical extracts

Ehab Mahran [a, b, c], Michael Keusgen [b], Gertrud E. Morlock [a, *]

[a] Institute of Nutritional Science, Chair of Food Science, Interdisciplinary Research Center IFZ, Justus Liebig University Giessen, Heinrich-Buff-Ring 26-32, 35392, Giessen, Germany
[b] Institute of Pharmaceutical Chemistry, Philipps University Marburg, Marbacher Weg 6-10, 35032, Marburg, Germany
[c] Pharmacognosy Department, Faculty of Pharmacy, Al-Azhar University, 11371, Cairo, Egypt

ARTICLE INFO

Article history:
Received 1 November 2019
Received in revised form
13 January 2020
Accepted 17 January 2020
Available online 21 January 2020

Keywords:
β-Glucuronidase inhibition
Effect-directed analysis
Silymarin
Primula
Silychristin
Flavonoids

ABSTRACT

The inhibition of the β-glucuronidase released from gut bacteria is associated with specific health-related benefits. Though a number of β-glucuronidase inhibition assays are currently in use, none of them can directly measure the relevant activity of each single constituent in a complex mixture, without prior separation and tedious isolation of the pure compounds. Thus, the hyphenation of the high performance thin layer chromatography (HPTLC) technique with a β-glucuronidase inhibition assay was investigated and successfully demonstrated for the first time. A colorimetric as well as fluorometric detection of the inhibitors was achieved using 5-bromo-4-chloro-3-indolyl-β-D-glucuronide as a substrate. Hence, β-glucuronidase inhibitors were detected as bright zones against an indigo blue or fluorescent background. The established method was optimized and validated employing the well-known inhibitor D-saccharic acid 1,4-lactone monohydrate. As proof of concept, the suitability of the new workflow was verified through analysis of two botanical extracts, *Primula boveana* and silymarin flavonolignans from *Silybum marianum* fruits. The found inhibitors were identified by spectroscopic methods; one of them, 3′-*O*-(β-galactopyranosyl)-flavone, is here described as a newly isolated natural compound. The new hyphenation HPTLC-UV/Vis/FLD-β-glucuronidase inhibition assay-HRMS covers four orthogonal dimensions, *i.e.* separation, spectral detection, biochemical activity and structural characterization, in a highly targeted time- and material-saving workflow for analysis of complex or costly mixtures.

1. Introduction

A large number of xenobiotics are eliminated from the body by glucuronidation, which is a fundamental phase II metabolic reaction. Compounds or intermediate metabolites harboring functional groups, like OH, COOH, or NH_2 on their structures, are normally marked for elimination *via* the glucuronidation pathway [1]. Nevertheless, this detoxification process could be hampered in the intestine by the reverse deglucuronidation reaction, mediated by the β-glucuronidase from opportunistic enterobacteria, *e.g. E. coli* [2,3]. This retroverted process was defined as the underlying cause of several diseases, *e.g.* irinotecan-induced severe diarrhea and NSAID-associated serious intestinal injury [4,5]. Also, the aggravated deleterious effects of many food-borne carcinogens like heterocyclic amines [6] are due to this deglucuronidation process, a prominent example is the enhanced genotoxicity of 2-amino-3-methylimidazo[4,5-f]quinolone [7]. The bacterial β-glucuronidase has also been linked to the increased incidence of the colon cancer [8] and Crohn's disease [9]. Crystal structure analysis of the complexes between inhibitors and β-glucuronidase from *E. coli* revealed that the bacterial β-glucuronidase encompasses a unique loop that is missing in the mammalian one. The emerged selective inhibitors of the bacterial ortholog preferentially bind to this loop [10]. Deficiency, and in deed inhibition, of the human β-glucuronidase correlated with health risks, *e.g.* Sly syndrome or mucopolysaccharidosis type VII disease [11]. Thus, it becomes obvious that inhibition of the gut bacterial β-glucuronidase, rather than the mammalian ortholog, would carry diverse health benefits. Recently, many research trendlines have been focusing on the development of drug molecules capable of inhibiting solely the bacterial β-glucuronidase, but not the mammalian ortholog [12,13]. The β-glucuronidase inhibition has also been linked to some

* Corresponding author.
E-mail address: gertrud.morlock@uni-giessen.de (G.E. Morlock).

https://doi.org/10.1016/j.acax.2020.100039

hepatoprotective activities of some plants [14,15]. A strong clue of the hepatoprotective potential of β-glucuronidase inhibitors has also been determined for the lactic acid bacteria, a potent inhibitor of β-glucuronidase of the intestinal microflora [16].

Principally, the detection and evaluation of the β-glucuronidase activity depends on the potential of the enzyme to selectively hydrolyze a number of readily available chromogenic [17–19] or fluorogenic [20] substrates. Nevertheless, when applied to complex mixtures [14,15,21,22], these assays could only point to the activity of the entire mixture without instantaneous reference to the activity of individual constituents, unless purified before. In most cases, such assays follow extensive time-, chemicals- and materials-consuming procedures. Bringing these concerns together, the development and establishment of the β-glucuronidase inhibition assay incorporated into a chromatographic screening would allow a straightforward evaluation of complex samples with regard to individual inhibitors.

So far, such a HPTLC-β-glucuronidase assay has not been reported among the hyphenations of other biochemical hydrolase assays (*e.g.*, α- and β-glucosidase [23], acetyl- and butyrylcholinesterase [24] and lipase [25] assays) with high performance thin layer chromatography (HPTLC). The piezoelectric spraying of bacterial and enzymatic assay solutions was recently reported and discussed among others to need less volume of the enzyme solution, if compared to the currently used immersion technique [26]. HPTLC coupled to powerful structural elucidation methods, such as high-resolution mass spectrometry (HRMS), UV/Vis/FLD detection and FTIR spectroscopy, enabled the tentative compound assignment by exploiting different orthogonal dimensions [27–29].

Inspired by all these considerations, we targeted to hyphenate HPTLC with the β-glucuronidase inhibition assay, presented in this study for the first time. Different options were discussed for the detection of β-glucuronidase inhibitors. The HPTLC-β-glucuronidase inhibitor assay was developed, optimized and verified using extracts of *Primula boveana* and flavonolignans from *Silybum marianum* fruit extract. The detected β-glucuronidase inhibitors were identified by HPTLC-HESI-HRMS/MS and NMR analysis.

2. Materials and methods

2.1. Materials

HPTLC plates silica gel 60 with and without F_{254} (20 cm × 10 cm) were obtained from Merck (Darmstadt, Germany). *Primula boveana* Decne. ex Duby leaves were collected from Saint Catherine area in Egypt. Solvents (HPLC grade) obtained from Thermo Fischer Scientific (Schwerte, Germany). β-Glucuronidase type VII-A from *E. coli* (5 kU) and silymarin flavonolignans subfraction powder (SF) of *Silybum marianum* plant (fruit and root) were obtained from Sigma Aldrich (Taufkirchen, Germany). 5-Bromo-4-chloro-3-indolyl-β-D-glucuronide (X-Gluc) was purchased from Carbosynth (Berkshire, UK) and D-saccharic acid-1,4-lactone monohydrate (SL) was obtained from Santa Cruz Biotechnology (Heidelberg, Germany). Bovine serum albumin (BSA, Albumin Fraction V), natural product reagent (NP), polyethylene glycol (PEG), and potassium phosphate buffer salts (K_2HPO_4 and KH_2PO_4) were from Carl Roth (Karlsruhe, Germany). Distilled water was produced by the Heraeus Destamat Bi-18E distillator (Thermo Fisher Scientific, Schwerte, Germany).

2.2. Solutions and botanical extracts

Each of SL (1 mg mL^{-1}) and X-Gluc (2 mg mL^{-1}) were dissolved in distilled water. β-Glucuronidase solution (25 U mL^{-1}) was prepared in potassium phosphate buffer (0.1 M, pH 7.0), containing 0.1% BSA. Extract of *Primula boveana* was prepared by extracting 1 g of the finely powdered, air-dried leaves with 80% methanol (1:10, *W/V*) for 24 h. The resulting extract was filtered through a syringe filter (0.45 μm, Chromafil, Carl Roth, Germany) and kept at −20 °C until analysis. Flavone and 2′-methoxyflavone were previously isolated from the same plant and dissolved in methanol (1 mg mL^{-1}) [29]. As a ready-to-obtain mixture of the major flavonolignans in the milk thistle (*Silybum marianum*) fruit, the commercially available SF powder (250 mg) was dissolved in 2.5 mL methanol by sonication for 10 min and diluted with methanol (1:100, *V/V*), followed by membrane filtration of an aliquot into the sampler vial (0.45 μm).

2.3. HPTLC-UV/Vis/FLD-β-glucuronidase inhibition assay

The SL solution (1 mg mL^{-1}, 1.0 μL per band, *i.e.* 1 μg per band) as well as *Primula boveana* (100 mg mL^{-1}, 0.5 or 1.0 μL per band, *i.e.* 50 or 100 μg per band) and *Silybum marianum* SF extracts (1 mg mL^{-1}, 1.0 μL per band, *i.e.* 1 μg per band) were applied as 8 mm band using the Automatic TLC Sampler (ATS 4, CAMAG, Muttenz, Switzerland). All mobile phases used in this study are prepared in volumetric ratios. The *Primula boveana* extract was separated using two different mobile phases, n-hexane - ethyl acetate (7:3) and ethyl acetate - methanol - water - formic acid (8:1:0.4:0.1). The *Silybum marianum* SF extract was studied using two different mobile phases either chloroform - acetone - formic acid (75:16.5:8.5) or toluene - ethyl acetate - formic acid (9:6:0.4). The chromatogram was documented under white light illumination, UV 254 nm and UV 366 nm using the TLC Visualizer (CAMAG). All assay solutions were piezoelectrically sprayed using the green nozzle generating the smallest droplet size (finest spray; nozzle mesh size 4–5 μm) and using the shortest spraying time (fastest speed at spray level 6), if not stated otherwise (TLC Derivatizer, CAMAG). Developed plates were dampened (pre-wetted) by spraying with 0.5 mL potassium phosphate buffer (0.1 M, pH 7.0). For plates developed in an acidic mobile phase, neutralization was achieved by spraying 2.0 mL potassium phosphate buffer (0.1 M, pH 7.8) after the pre-wetting step. Afterwards, 3.0 mL of β-glucuronidase solution were sprayed and plates were horizontally positioned in a humid box and incubated at 37 °C for 15 min. After incubation, 1.5 mL of the X-Gluc substrate solution (2 mg mL^{-1}) were sprayed (red nozzle generating the largest droplet size; nozzle mesh size 9–12 μm) and incubated at 37 °C for 1 h. The β-glucuronidase inhibition was documented under white light illumination and UV 366 nm using the TLC Visualizer (CAMAG). The UV/Vis absorbance spectrum was recorded from 200 to 800 nm on the colored background, while the colorless SL inhibition zone served as background reference. The absorbance measurement was performed at 612 nm employing an inverse scanning strategy (trick to avoid peak conversion to negative peaks by selecting the software parameter fluorescence mode without optical filter; TLC Scanner 4, CAMAG).

2.4. Post-chromatographic derivatization via NP/PEG reagent

Developed plates were heated on the TLC Plate Heater III (CAMAG) at 100 °C for 3 min. After cooling, plates were dipped in the NP reagent (0.5% in ethyl acetate, immersion time 0 s, immersion speed 5 cm s^{-1}) using the Chromatogram Immersion Device). After drying, plates were immersed in the PEG solution, (5% in methylene chloride). The plates were heated at 100 °C for 5 min and chromatograms were documented at UV 366 nm.

2.5. Isolation and identification of compound P3

Compound **P3** was isolated from *Primula boveana* total extract

by means of preparative HPLC. Separation was achieved on an RP-column (250 mm, ID 21 mm, 5 μm Nucleodur C18, Macherey-Nagel, Düren, Germany) using the DeltaPrep chromatography system equipped with a dual wavelength absorbance detector set to 254 nm and controlled by MassLynx V4.1 software (Waters, Milford, MA, USA). The extract was manually injected in aliquots of 200 μL (10 mg mL^{-1}). Compound **P3** was separated by isocratic elution with 40% methanol in water pumped at 7.0 mL min^{-1}. Fractions containing **P3** were pooled and evaporated at 40 °C under reduced pressure to afford **P3** (6 mg) as yellowish brown powder. The UV measurement was done on UV-2401PC spectrophotometer (Shimadzu, Kyoto, Japan) and IR spectrum was collected on Bruker Alpha IR spectrometer (Bruker, Hamburg, Germany). NMR data were acquired on ECA500 spectrometer (JEOL, Tokyo, Japan).

2.6. Acid hydrolysis of compound P3

For determination of the hexose moiety of **P3**, acid hydrolysis was performed [30]. **P3** (1 mg) was dissolved in 1% sulphuric acid (200 μL) and heated at 95 °C in a block heater for 1 h. Then, the solution was partitioned twice with ethyl acetate (300 μL). The aqueous layer, after separation of the organic layer, was neutralized with sodium carbonate (1 M). The sugar was determined by co-chromatographic TLC analysis with reference galactose (1 mg mL^{-1} in water) and glucose (1 mg mL^{-1} in water).

2.7. Statistical analysis

Using the Minitab software (Minitab, State College, PA, USA), collected data were subjected to analysis of variance and means were compared through Fisher Pairwise Comparison ($p \leq 0.05$).

2.8. HPTLC-HRMS/MS

The plate was pre-washed with methanol - formic acid 10:1, *V/V*, then acetonitrile - methanol 2:1, *V/V*, and each time, dried at 100 °C for 20 min [31]. After analysis of the *Silybum marianum* SF extract, the β-glucuronidase inhibitors were marked at UV 254 nm. Target bands were eluted with methanol (0.1 mL min^{-1}) by the Plate Express interface (Advion, Ithaca, NY) into the QExactiveTM PlusHybrid Quadrupole-Orbitrap mass spectrometer (Thermo Fisher Scientific, Dreieich, Germany) equipped with a heated electrospray ionization source. The full scan HRMS data (*m/z* 100−1000) was acquired in the negative ion mode with the following settings: capillary voltage −3.0 kV, probe temperature 200 °C and resolution 280 000. Nitrogen was the sheath and aux gas. The HRMS/MS data was obtained by selected reaction monitoring, for which the inclusion list was generated via the targeted precursor ions with an isolation window of *m/z* 0.4 at a resolution of 35 000 over a range of collision energies (10−50 V). Data acquisition and processing were controlled by Xcalibur 3.0.63 software.

3. Results and discussion

3.1. Development of a planar/in situ β-glucuronidase assay

The transfer of microtiter plate assays for β-glucuronidase inhibition to HPTLC and the optimization for its planar application were investigated. After selection of the detection principle, the detection wavelength, enzyme concentration, reaction time, and the effect of using HPTLC plates with or without fluorescence indicator were studied. For all of these parameters, the reaction temperature for the β-glucuronidase was kept at 37 °C [32−34]. An aqueous solution of the most widely used β-glucuronidase reference inhibitor SL was used. The peak areas of the inhibition zones were used as a criterion for optimization of the experimental parameters. For the *in situ* detection on the plate, 5-bromo-4-chloro-3-indolyl-β-D-glucuronide (X-Gluc) [32] was selected as substrate for the β-glucuronidase (Fig. 1). A number of further substrates are available at relatively lower prices, however, generate a weaker contrast of the inhibition zone to the plate background (*e.g.,* a colorless inhibition zone on a yellow colored background for *p*-nitrophenyl-β-D-glucuronide) and provide a single detection mode only (*e.g.,* either absorbance using naphthol β-D-glucuronide or fluorescence using 4-methylumbelliferyl β-D-glucuronide). As the detection can be interfered by natively colored/fluorescent compounds (*e.g.,* alkaloids and flavonoids), the indigo blue color formation using the X-Gluc was found to be advantageously, as this blue color nuance is normally not found in natural food.

The active inhibitors were detectable as colorless (white) spots against an indigo blue background, permitting their colorimetric detection. Although X-Gluc was used as chromogenic substrate for detection by absorbance [35,36], its fluorometric detection is also feasible due to the fluorescent intermediates formed during the enzymatic reaction. Similarly to the acetylcholineesterase inhibition assay using indoxyl acetate as substrate [37], the X-Gluc substrate provided a dual fluorometric/colorimetric readout of the biochemical signal. All assay solutions were studied to be sprayed piezoelectrically on the HPTLC plate for a material/cost-saving workflow, as expensive enzymes cause high prices of enzymatic assays. By doing so, 3.0 mL of β-glucuronidase solution (25 U mL^{-1}) were sufficient for covering a plate size of 20 cm × 10 cm. When compared to the status quo, automated immersion required *ca.* 70 mL enzyme solution, although it was reusable for several times.

The visual evaluation and documentation were performed as dual fluorometric/colorimetric readout. For densitometry, absorbance measurement was preferred to the more sensitive fluorescence measurement, as it was more selective with regard to the natively colored/fluorescent compounds in the extracts. The optimum detection wavelength was found to be in the broad absorbance maximum between 610 - 660 nm as deduced from the UV/Vis spectrum (Fig. S-1). This optimum range was in agreement to the visible detection of the indigo blue [38]. As a proof of the proper detection wavelength selection, the plates were scanned at a lower (612 nm) and a higher wavelength (650 nm). The statistical analysis ($p \leq 0.05$) showed no significant difference between both measured peak areas ($n = 3$), indicating that any of these wavelengths in the plateau can be used as an optimum wavelength for the densitometric measurement, as expected.

For determination of the optimum enzyme concentration, a range of β-glucuronidase concentrations between 2 and 33 U mL^{-1} was investigated. By piezoelectric spraying of 3.0 mL enzyme solution over a 200-cm^2 area, the β-glucuronidase surface coverage was between 0.03 and 0.5 U cm^{-2}. The optimum β-glucuronidase concentration was determined as 25 U mL^{-1}, equal to a surface coverage of 0.375 U cm^{-2} (Fig. 2A). This *in situ* assay required much lower amounts of the enzyme, as 75 U were sufficient to spray on an HPTLC plate (20 × 10 cm), on which, for example, 20 or 40 samples (bandwise or spotwise) can be separated in parallel pointing to individual inhibiting compounds therein. If a chromatographic separation is not targeted for screening of single compounds (applying the sample mixture as a whole), up to 120 samples can be applied (*e.g.*, as 8-mm bands) using the FreeMode option of the ATS4 device. In contrast, a wide range of enzyme concentrations was reported for status quo *in vitro* assays, ranging from 167 U (β-glucuronidase type B-1 from bovine liver) [22] and 99 U (β-glucuronidase from bovine liver) [15] to 2 U (β-glucuronidase from *E. coli*) [34] for each microtiter plate well. If compared to the lowest consumption per 96-well plate (192 U), the enzyme consumption of 75 U per HPTLC plate is by 60% lower and even

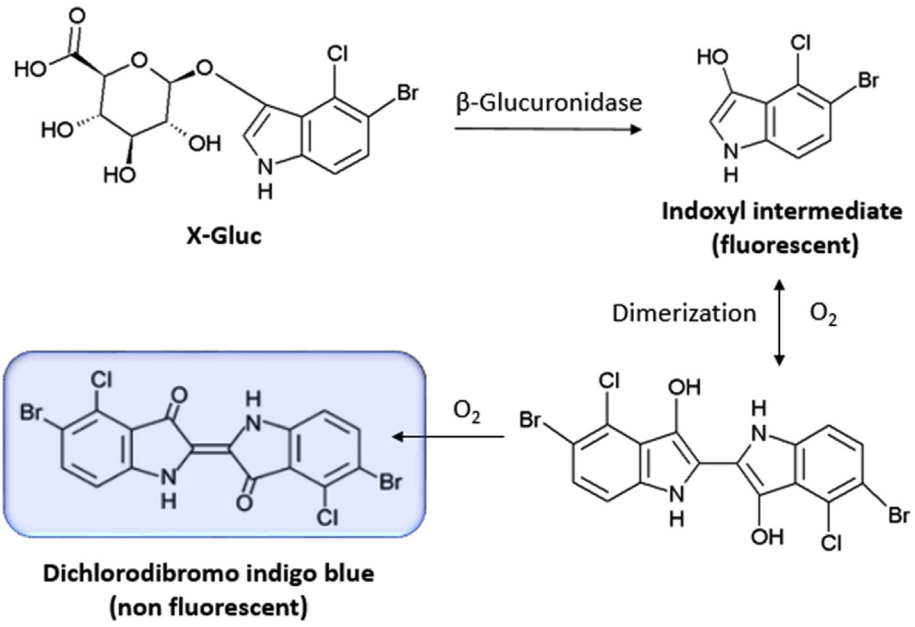

Fig. 1. Enzymatic reaction of the β-glucuronidase using X-Gluc as a substrate.

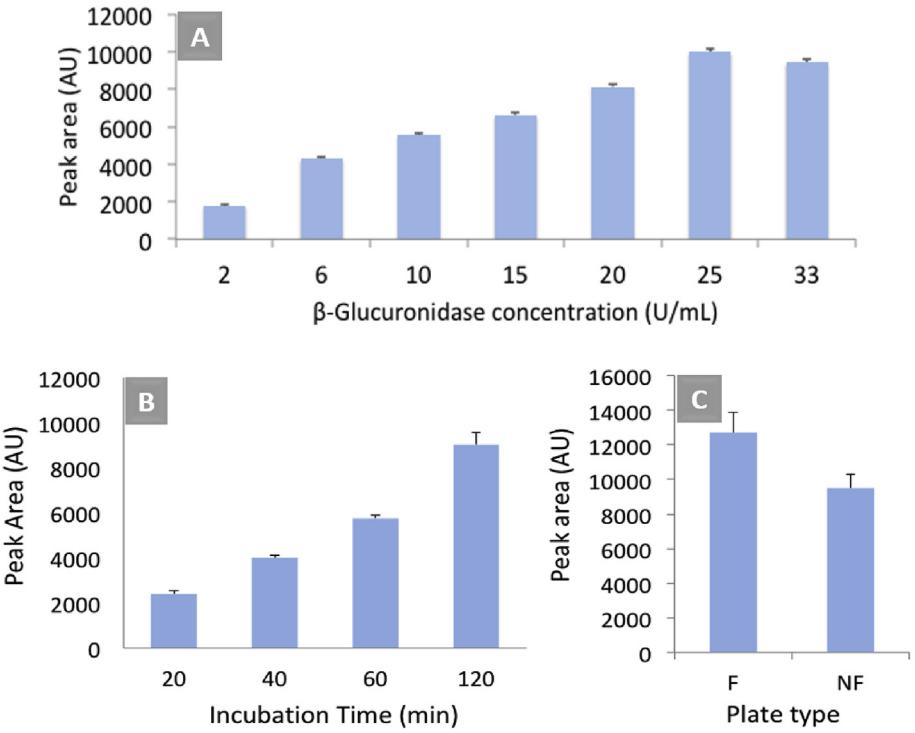

Fig. 2. Effect of β-glucuronidase concentration (A), incubation time (B) and plate type (with fluorescence indicator F *versus* without NF; C) on peak areas of the reference inhibitor SL (1 μg/band applied, $n = 3$, absorbance measurement at 612 nm).

much lower, if mixtures are separated by column chromatography with each fraction or compound subjected to the assay.

With regard to the reaction time, 20, 40, 60 and 120 min were studied (Fig. 2B), as most *in vitro* β-glucuronidase inhibition assays used 0.5–1 h, terminated by alkali addition [14,15,21,33]. The reaction time of 60 min turned out to be a good compromise. The LOD was found to be sufficient to detect middle to strong inhibitors. Though the inhibition was also detectable at shorter reaction times (*i.e.* 30 min), the contrast of the inhibition band to the background was weaker. Although the response was still improved by a longer reaction time of 120 min (statistically proven by $p \leq 0.05$), it was decided against, for the sake of a short workflow. The addition of pro-oxidants or oxidation catalysts, *e.g.* potassium ferricyanide, to the reaction mixture could accelerate the rate of the colored end product formation, however, needs to be studied first to avoid a loss of the enzymatic activity.

The influence of the fluorescent indicator on the colorimetric detection was studied using two types of the HPTLC plates, *i.e.* with and without fluorescent indicator (Fig. 2C). The statistical comparison of the results showed a significantly increased signal of the peak areas on HPTLC plates with fluorescent indicator. Hence, HPTLC plates with fluorescent indicator were preferred for this assay.

3.2. Validation of the new planar/in situ β-glucuronidase assay

The new planar β-glucuronidase inhibition assay was validated with regard to the limit of detection (S/N ≥ 3), working range and specificity. Different volumes of the SL solution were applied (0.75–2000 ng/band, $n = 3$ plates, representative replicate in Fig. 3). The peak area of the inhibition zone of each amount was obtained after densitometric measurement at 612 nm. For the 62-ng band of SL, a S/N 4.5 was achieved (mean peak area 374 ± 85 AU). Thus, the limit of detection of SL was below 62 ng/band. The selected working range between 62 and 1000 ng per band led to a second order polynomial equation ($y = -0.004x^2 + 8.400x + 22.69$, $R^2 = 0.993$). The specificity of the β-glucuronidase to X-Gluc was confirmed using a different substrate (2-naphthyl-β-D-glucopyranoside), which carried a closely related but glycosyl moiety. Its solution was piezoelectrically sprayed (2.0 mL, 0.1% ethanolic solution mixed 9:1 with 10 mM aqueous sodium chloride solution), followed by 0.75 mL of a 0.4% aqueous Fast Blue B salt solution. After incubation, the absence of the indigo blue dye color confirmed the specificity of the β-glucuronidase towards the X-Gluc substrate.

3.3. Integration of the planar assay and application of the HPTLC-UV/Vis/FLD-β-glucuronidase assay to two botanicals

The newly developed workflow for the planar β-glucuronidase assay (*in situ* the adsorbent) was integrated into the HPTLC workflow (Fig. 4). As proof of principle and for verification of the newly developed protocol, complex sample mixtures were targeted. Plants accumulating numerous metabolites with variable physical and chemical properties are regarded as indispensable source of many potent therapeutic agents [39], and among these, *Primula boveana* leaf extract and *Silybum marianum* SF extract were selected, and after optimization of the chromatographic system, successfully applied to the newly developed workflow as illustrated (Fig. 4).

The studied *Primula boveana* plant is rare and only a very low extract volume was provided after the already performed effect-directed analyses [29]. The newly developed HPTLC-UV/Vis/FLD-β-glucuronidase inhibition assay was suited best, as other techniques of effect-directed analysis (*e.g.*, in the microtiter plate) were not capable to cope with that low volume. By such an *in situ* assay on a solvent-free chromatogram, the contact of all separated compounds with the enzyme solution was ensured. Thus, an inefficient dissolution of non-polar compounds that may occur in the aqueous enzyme solution was excluded, which was also a crucial aspect with regard to the costly extract. The *Primula boveana* extract solution was applied on an HPTLC plate silica gel 60 F_{254} and separated with *n*-hexane – ethyl acetate, 7:3 (Figs. 3B and 5). The residual solvent traces were removed from the HPTLC plate using the drying option of the ADC2 system for 20 min. The neutralization step was not performed, as it was only needed for acidic (or alkaline) mobile phases. After application of the planar assay, two non-polar metabolites (**P1** and **P2**) distinctly inhibited the β-glucuronidase (Figs. 3B and 5A, tracks 4 and 5).

The *Silybum marianum* SF extract solution was applied on an HPTLC plate silica gel 60 F_{254} (Fig. 4). The influence of two different mobile phases on the result was studied. These two mobile phases were previously shown to separate the flavonolignan constituents of *Silybum marianum* [40,41]. The residual solvent traces were removed from the HPTLC plate using the drying option of the ADC2 system for 20 min. For the given acidic mobile phases, the plates were also studied with *versus* without prior neutralization. Upon using a mixture of chloroform, acetone and formic acid as mobile phase containing 8.5% formic acid (Fig. 6A), the assay did only work when the plate was neutralized before (tracks 5 *versus* 6). In contrast, on the plate developed with toluene, ethyl acetate and formic acid containing 2.6% formic acid (Fig. 6B), the β-glucuronidase inhibition signal was revealed in the autogram (track 6). As observed for the separation of both plant samples, the current assay can tolerate formic acid traces to a certain extent. Nevertheless, the application of the neutralization step is recommended, as with neutralization of the plate, the signal intensity was best (tracks 5). Though the use of an acidic mobile phase was indispensable for a good separation of the active metabolites, the acid was a serious issue for the enzymatic assay hyphenated to planar

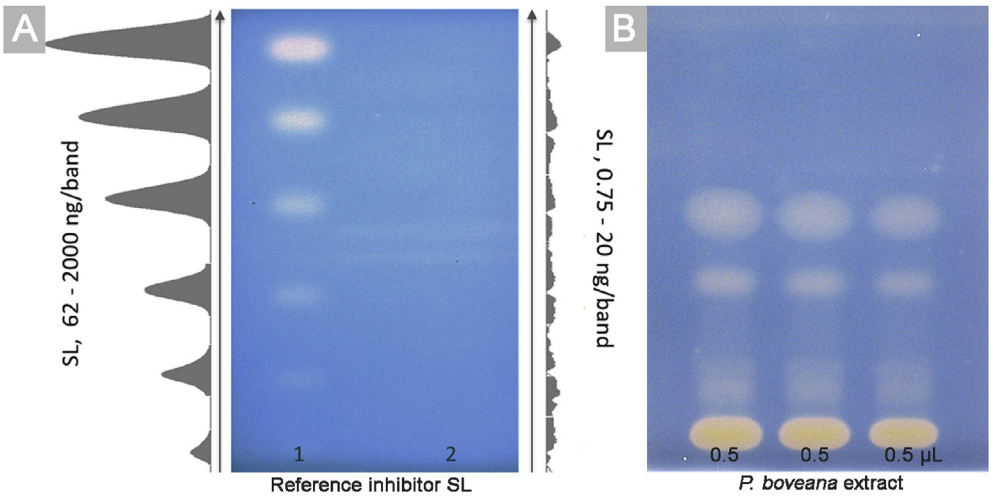

Fig. 3. Limit of detection of the colorimetric planar β-glucuronidase assay for the reference inhibitor SL ranged 0.75–2000 ng/band (A; track patterns 1 and 2) and absorbance measurement at 612 nm; final HPTLC-β-glucuronidase inhibition assay applied to *Primula boveana* leaf extract (B; 100 mg mL^{-1}, 0.5 µL/band applied, $n = 3$), both documented under white light illumination (reflectance mode).

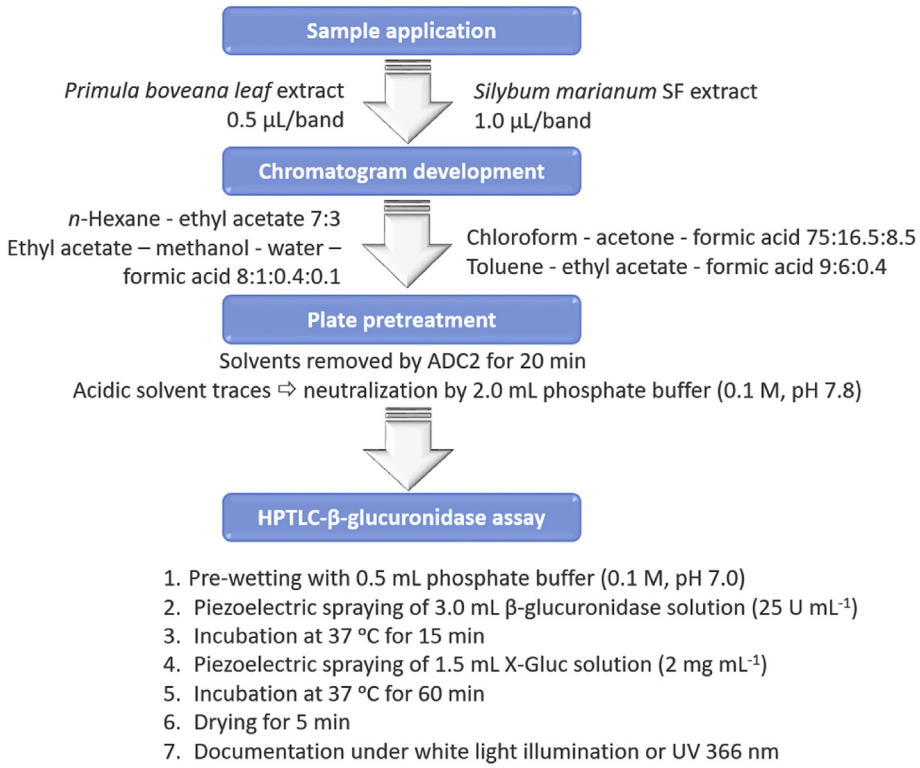

Fig. 4. Schematic representation of the newly developed workflow for the *in situ* HPTLC-β-glucuronidase inhibition assay as applied to *Primula boveana* leaf extract and *Silybum marianum* SF extract.

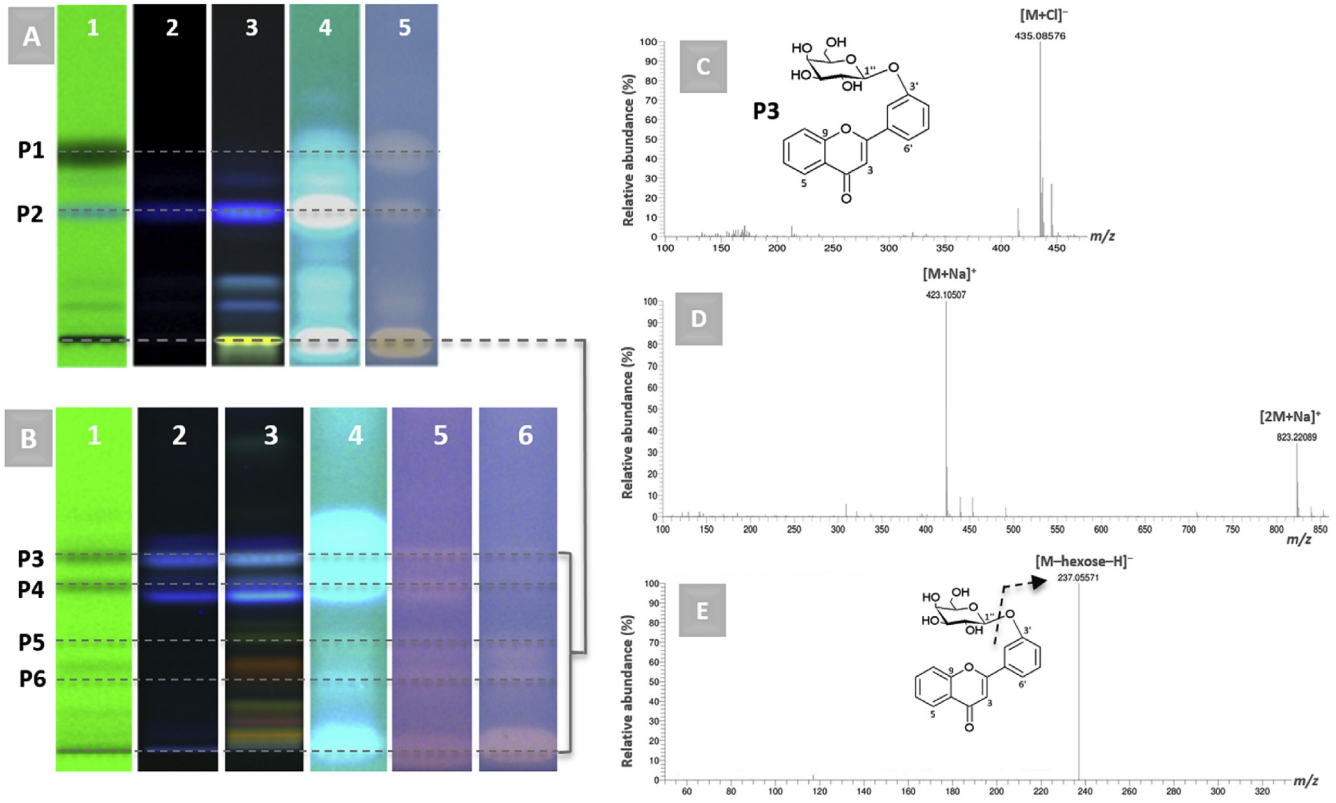

Fig. 5. New HPTLC-β-glucuronidase assay for detection of inhibitors in *Primula boveana* leaf extract (100 mg mL^{-1}) developed with *n*-hexane – ethyl acetate, 7:3 (A, 0.5 µL/band) and ethyl acetate – methanol – water – formic acid, 8:1:0.4:0.1 (B, 1.0 µL/band), detected at UV 254 nm (1), 366 nm (2) and 366 nm after NP/PEG derivatization (3) as well as after the assay, at UV 366 nm (4) and white light illumination without (5) and with prior neutralization (6). HPTLC-HESI-HRMS spectra of the newly found inhibiting compound **P3** in the negative (C) *vs.* positive (D) ionization mode as well as its respective HRMS/MS spectrum (E).

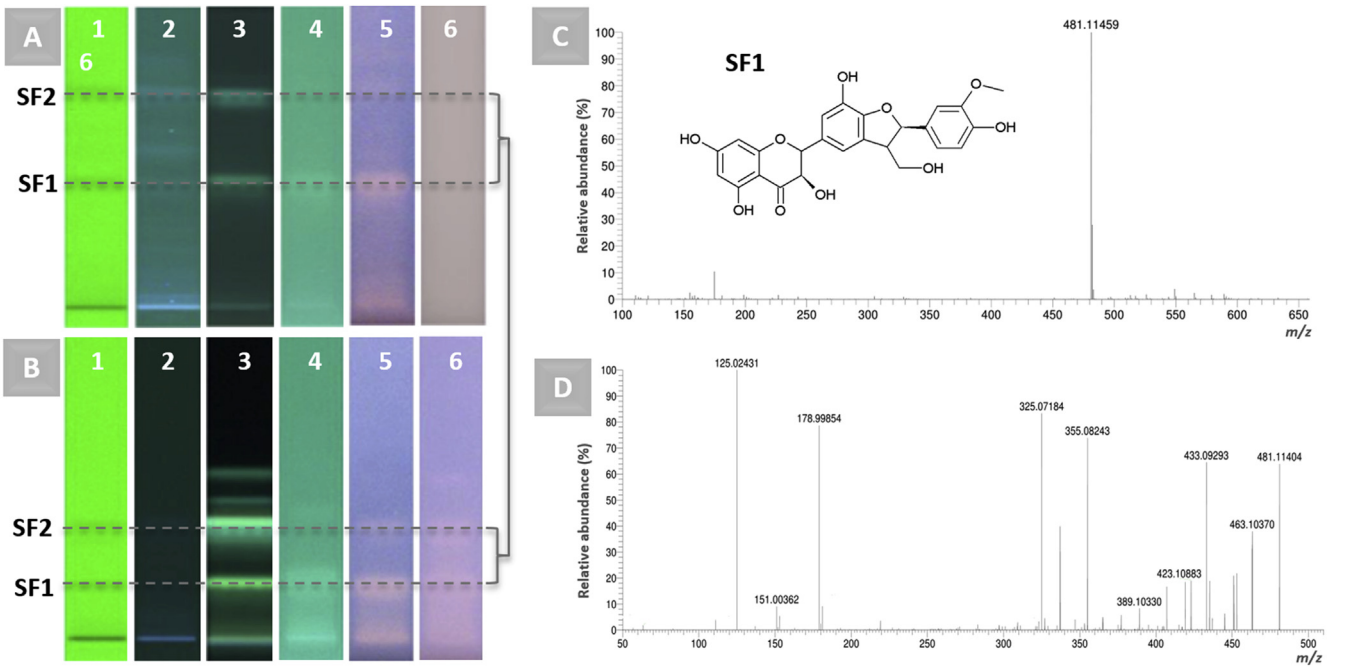

Fig. 6. New HPTLC-β-glucuronidase assay for detection of inhibitors in *Silybum marianum* SF extract (1 mg mL^{-1}; 1.0 μL/band) developed with chloroform – acetone - formic acid, 75:16.5:8.5 (A) and toluene - ethyl acetate – formic acid, 9:6:0.4 (B), detected at UV 254 nm (1), 366 nm (2) and after NP/PEG derivatization (3) as well as after the assay, at UV 366 nm (4) and white light illumination (5) and same without neutralization (6). HPTLC-HESI-HRMS spectrum of the found inhibitor **SF1** (C) and its respective HRMS/MS spectrum (D).

chromatography. Despite extended plate drying after the development (20 min), the residual acids remained on the plate. These were difficult to remove with conventional drying techniques, *e.g.*, using a hair dryer or the drying option of the ADC2 system. Hence, when developed with an acidic mobile phase, the neutralization of the chromatogram was crucial for the successful performance of this newly developed assay. This recommendation was in accordance with previous studies. For example, a phosphate buffer (0.2 M, pH 7.8) ensured the optimum pH 7 of the plate for the following microbial and enzymatic *in situ* assays [42]. Or, the plate was neutralized by immersion into a 2% sodium hydroxide solution for the successful enzymatic assay performance [43].

3.4. Characterization of β-glucuronidase inhibitors in Primula boveana leaf extract by HESI-HRMS/MS and 1D/2D NMR analysis

The HPTLC-UV/Vis/FLD-β-glucuronidase assay revealed two non-polar β-glucuronidase inhibitors (**P1** and **P2,** Fig. 5A, tracks 4 and 5), which were identified as flavone compounds, namely, flavone (**P1**) and 2′-methoxyflavone (**P2**). Identification was performed by co-chromatography of the respective reference compounds on the HPTLC plate (Fig. S-2). These were previously isolated from the same plant and then characterized by HPTLC-HESI-HRMS and NMR [29]. Flavonoids are known to inhibit many enzymes [44], and our findings demonstrate their potential activity as β-glucuronidase inhibitors. In a previous study [33], scutellarein and luteolin, two flavone-type flavonoids, were found as potent β-glucuronidase inhibitors and their activity was defined as higher than the reference inhibitor SL.

At the start zone, there was also observed a strong inhibition, which was worth investigating. Therefore, a mobile phase of a higher elution power was used, *i.e.* ethyl acetate – methanol - water - formic acid (8:1:0.4:0.1). As an acidic mobile phase, the developed plates were evaluated without *versus* with prior neutralization by phosphate buffer (piezoelectric spraying of 2.0 mL, 0.1 M, pH 7.8). Four major β-glucuronidase inhibitors (**P3**–**P6**) were observed (Fig. 5B). The HPTLC-HRMS and -HRMS/MS data for compounds **P3**–**P6** were recorded in the negative ionization mode.

Compound **P3** displayed a mass signal at *m/z* 435.08576 (Fig. 5C), indicating a molecular formula of $C_{21}H_{20}O_8$ (calculated *m/z* 435.08522 for $[M+Cl]^-$). In HPTLC-MS, a chlorine adduct can be caused by the surrounding atmosphere or from residual chlorinated solvent traces in the instrumental system (from prior users) [45,46]. For confirmation of the molecular formula, the measurement was performed in the positive ion mode (Fig. 5D), which showed mass signals at *m/z* 423.10507 $[M+Na]^+$ and 823.22089 $[2\ M + Na]^+$. In the HPTLC-HRMS/MS spectrum of **P3** (Fig. 5E), a single fragment ion at *m/z* 237.05571 indicated a loss of 162 Da attributable to a hexose unit. So, the aglycone was suggested to be a monohydroxyflavone (calculated *m/z* 237.05572 for $[M\text{-hexose-H}]^-$) and the structure of **P3** as flavone-*O*-hexoside. A metabolite of such structural formula has not been reported previously in any of the *Primula* species. Therefore, priority was given to fully elucidate the structure of this compound. After isolation, UV, IR, 1D and 2D NMR measurements of **P3** were acquired. UV (MeOH, Fig. S-3): were at 218, 260 and 306 nm. The IR bands were at 3358, 2924, 1650, 1604, 1380 and 1075 cm-1 (Fig. S-4). For the 1D NMR experiments, the spectra were first collected in CD_3OD and DMSO-d_6 (Table 1) to avoid overlapping by the water signal and for better determination of the coupling constants. The ^1H, ^{13}C, COSY, and HSQC NMR spectra (Figs. S-5 to S-10) indicated that **P3** is a flavonoid compound. The presence of a singlet proton at δ_H 7.0 (H-3) attached to a carbon at δ_C 107.7 (C-3), confirmed that **P3** is a flavone-type flavonoid. The lack of ring-B symmetry as well as observation of all proton/carbon signals of ring A (Table 1), suggested that the sugar unit is positioned in ring B. The observed chemical shifts for ring B of **P3** were comparable to those reported for 3′-*O*-hexosyl-substituted flavonoids [47]. The acid hydrolysis experiment confirmed that galactopyranosyl is the hexose sugar of **P3**. It possessed a β-configuration from the coupling constants of its

Table 1
^{1}H and ^{13}C NMR data of **P3** collected in CD_3OD and DMSO-d_6.

Position	In CD_3OD		In DMSO-d_6	
	δ_H multiplicity (J in Hz)	δ_C	δ_H multiplicity (J in Hz)	δ_C
2	–	163.9	–	162.8
3	6.93 s	106.6	7.02 s	107.7
4	–	179.4	–	177.6
5	8.13 dd (1.6, 8.1)	124.7	8.03 ddd (0.5, 1.6, 8.1)	125.3
6	7.51 ddd (1.1, 7.1, 8.1)	125.4	7.47 m	126.1
7	7.83 ddd (1.6, 7.1, 8.5)	134.4	7.81 m	134.9
8	7.76 ddd (0.5, 1.1, 8.5)	118.3	7.79 m	119.2
9	–	156.4	–	156.3
10	–	123.3	–	123.8
1′	–	132.7		133.0
2′	7.80 t (2.0)	114.5	7.71 m	114.5
3′	–	158.5	–	158.5
4′	7.34 ddd (1.0, 2.5, 8.3)	120.3	7.23 ddd (1.0, 2.5, 8.3)	120.5
5′	7.4 t (8.2)	130.0	7.49 m	130.7
6′	7.72 ddd (1.0, 2.0, 8.0)	120.2	7.72 m	120.4
1″	4.90[a]	101.2	4.98 d (8.0)	101.1
2″	3.49 m	73.6	3.29 m	73.8
3″	3.53 m	76.6	3.26 m	77.2
4″	3.38 m	70.1	3.10 m	70.4
5″	3.50 m	77.1	3.41 m	77.8
6a″	3.93 dd (2.4, 12.0)	61.3	3.72 dd (2.1, 11.6)	61.4
6b″	3.70 dd (6.4, 12.0)		3.45 dd (6.4, 11.6)	

[a] Overlapped.

anomeric proton at δ_H 4.9 (1H, d, $J_{1'',2''} = 8.0$, H-1″). Also, the HMBC cross peak (Fig. S-11) between this anomeric proton and δ_C 158.4 (C-3′) confirmed that the β-galactopyranosyl moiety is being attached to C-3′. Thus, the structure of **P3** was determined as 3′-*O*-(β-galactopyranosyl)-flavone, which is here reported as a newly isolated natural compound.

Compounds **P4**–**P6** were tentatively characterized as hexosyl-*O*-dihydroxyflavone (**P4**), [hexosyl-deoxyhexosyl]-*O*-tetrahydroxyflavone (**P5**), and [hexosyl-deoxyhexosyl]-*O*-pentahydroxyflavone (**P6**) based on HPTLC-HRMS and −HRMS/MS data (Figs. S-12 to S-14) and/or co-chromatographic studies (Fig. S-15). Their HRMS mass spectra showed either deprotonated or chlorinated adduct signals as their molecular ion peaks. Also, HPTLC-HRMS/MS spectra displayed diagnostic signals due to loss of hexose (**P4**) or hexose + deoxyhexose (**P5** and **P6**). Co-chromatographic analysis of the *Primula boveana* extract with two reference standards, kaempferol-3-*O*-rutinoside and rutin, confirmed that **P6** is rutin, which was previously identified in the genus [48].

3.5. Characterization of β-glucuronidase inhibitors in Silybum marianum SF extract by HESI-HRMS/MS

After the successfully performed HPTLC-UV/Vis/FLD-β-glucuronidase assay, a pronounced active β-glucuronidase inhibitor was evident (**SF1**, Fig. 6A and B, tracks 5). The characterization of this most active metabolite **SF1** was made by HPTLC-HRMS and −HRMS/MS. The molecular formula of **SF1** was $C_{25}H_{22}O_{10}$ as deduced from the observed deprotonated molecule at *m/z* 481.11459 $[M-H]^-$ (calculated *m/z* 481.11402, Fig. 6C). Distinguishing the individual flavonolignan isomers of silymarin is challenging, as they share the same molecular mass of 482 Da and an almost comparable fragmentation behavior [49]. However, the occurrence as well as relative abundance of some diagnostic fragments assisted in the identification of the major individual flavonolignan components of silymarin. Recently, their MS/MS characterization has been studied [50,51]. Some spectral criteria were established to facilitate a rapid identification of the SF constituents by assigning diagnostic peaks and their relative abundances in the MS/MS spectra obtained at defined collision energies. In our study, the MS/MS scan of **SF1** was acquired at six different collision energies (10, 20, 25, 30, 40, and 50 V, Fig. S-16). For **SF1** the fragment ions increased with the collision energy increase up to 20 V, at which the optimum fragmentation pattern was obtained. At higher energies of 25–50 V, only stable ions were detected. In the HPTLC-HRMS/MS spectrum of **SF1** collected at collision energy of 20 V (Fig. 6D), several diagnostic mass remarks were detected. For example, the base peak at *m/z* 125, the relative signal abundance of >1 of the ion at *m/z* 463 to that at *m/z* 453 and the very low abundance for the ion at *m/z* 301 (almost 1% or less) were observed. The structural assignment of these fragment ions has been previously proposed [52] and our findings were found to be qualifiers of the flavonolignan silychristin [49–52]. Thus, the active β-glucuronidase inhibitor **SF**1 was identified as silychristin. Additionally, a second weak inhibition band (**SF2**) was detected. It emitted a green fluorescence after derivatization with the NP/PEG reagent. The HPTLC-HRMS and −HRMS/MS data for this compound have also been collected (Fig. S-17). **SF2** showed a molecular ion peak at *m/z* 481.11459, suggesting a molecular formula of $C_{25}H_{22}O_{10}$ $[M-H]^-$, which is identical to **SF1**. Nevertheless, the tandem mass analysis (at a collision energy of 20 V) of this compound showed some discrepancies from that of **SF1**, manifested by the higher relative abundance of the mass signal at *m/z* 301 (around 50%). The obtained mass signals of **SF2** were in accordance with those reported for the known flavonolignan silybin [52]. Thus, the active β-glucuronidase inhibitor **SF2** was identified as silybin. To date, only a single study has reported the coupling of HPTLC to (bio)assays and mass spectrometry for profiling of the active metabolites in milk thistle [40]. Hence, our findings are considered as the first report on linking HPTLC to HRMS/MS for the analysis of SF. The obtained HPTLC-HRMS/MS data of silychristin may facilitate its direct characterization in the total milk thistle extract.

4. Conclusions

For the first time, a straightforward protocol that combined planar chromatography *in situ* with the planar β-glucuronidase inhibition assay has been described. The new method provided a dual colorimetric/fluorometric readout of the biochemical signal. Complex sample mixtures were analyzed in parallel and evaluated for the presence of β-glucuronidase inhibitors. The new hyphenation HPTLC-UV/Vis/FLD-β-glucuronidase assay-HESI-HRMS/MS covered four orthogonal dimensions at one go on the same plate, *i.e.* separation, spectral detection, biochemical activity and structural characterization. A detailed characterization of the major active inhibitors in the extracts of *Primula boveana* leaf and *Silybum marianum* SF powder was done by HPTLC-ESI-HRMS/MS. The developed method successfully led to the structural elucidation of a newly isolated natural compound from *Primula boveana*. The new workflow succeeded for the analysis of costly extracts of rare plants (providing only a very low extract volume as for the studied *Primula boveana*) and avoided the discrimination of analytes (that may occur by an inefficient dissolution of non-polar compounds in the aqueous enzyme solution). The milk thistle plant has a wide range of medicinal applications that may attract various field of research and the developed protocol may support future multidisciplinary research.

Declaration of competing interest

The authors declare that they have no known competing financial interests or personal relationships that could have appeared to influence the work reported in this paper.

CRediT authorship contribution statement

Ehab Mahran: Funding acquisition, Conceptualization, Methodology, Investigation, Writing - original draft. **Michael Keusgen:** Supervision, Conceptualization, Methodology, Resources, Writing - review & editing. **Gertrud E. Morlock:** Supervision, Conceptualization, Methodology, Data curation, Resources, Writing - review & editing.

Acknowledgments

E.M. is grateful for the Yousef Jameel Scholarship Fund to perform research at Philipps University Marburg and Justus Liebig University Giessen. Instrumentation was partially funded by the Deutsche Forschungsgemeinschaft (DFG, German Research Foundation) - INST 162/471-1 FUGG; INST 162/536-1 FUGG.

Appendix A. Supplementary data

Supplementary data to this article can be found online at https://doi.org/10.1016/j.acax.2020.100039.

References

[1] J.K. Ritter, Roles of glucuronidation and UDP-glucuronosyltransferases in xenobiotic bioactivation reactions, Chem. Biol. Interact. 129 (2000) 171–193.
[2] P. Dashnyam, R. Mudubuddla, T.J. Hsieh, T.C. Lin, H.Y. Lin, P.Y. Chen, C.Y. Hsu, C.H. Lin, β-Glucuronidases of opportunistic bacteria are the major contributors to xenobiotic-induced toxicity in the gut, Sci. Rep. 8 (2018) 16372.
[3] K.A. Biernat, S.J. Pellock, A.P. Bhatt, M.M. Bivins, W.G. Walton, B.N.T. Tran, L. Wei, M.C. Snider, A.P. Cesmat, A. Tripathy, D.A. Erie, M.R. Redinbo, Structure, function, and inhibition of drug reactivating human gut microbial β-glucuronidases, Sci. Rep. 9 (2019) 825.
[4] A.B. Roberts, B.D. Wallace, M.K. Venkatesh, S. Mani, M.R. Redinbo, Molecular insights into microbial β-glucuronidase inhibition to abrogate CPT-11 toxicity, Mol. Pharmacol. 84 (2013) 208–217.
[5] R.N. Carmody, P.J. Turnbaugh, Host-microbial interactions in the metabolism of therapeutic and diet-derived xenobiotics, J. Clin. Invest. 124 (2014) 4173–4181.
[6] J. Zhang, C. Lacroix, E. Wortmann, H.J. Ruscheweyh, S. Sunagawa, S.J. Sturla, C. Schwab, Gut microbial beta-glucuronidase and glycerol/diol dehydratase activity contribute to dietary heterocyclic amine biotransformation, BMC Microbiol. 19 (2019) 99.
[7] C. Humblot, M. Murkovic, L. Rigottier-Gois, M. Bensaada, A. Bouclet, C. Andrieux, J. Anba, S. Rabot, β-Glucuronidase in human intestinal microbiota is necessary for the colonic genotoxicity of the food-borne carcinogen 2-amino-3-methylimidazo[4,5-f]quinoline in rats, Carcinogenesis 28 (2007) 2419–2425.
[8] D.H. Kim, Y.H. Jin, Intestinal bacterial β-glucuronidase activity of patients with colon cancer, Arch Pharm. Res. (Seoul) 24 (2001) 564.
[9] K. Gloux, J. Anba-Mondoloni, Unique β-glucuronidase locus in gut microbiomes of Crohn's disease patients and unaffected first-degree relatives, PloS One 11 (2016), e0148291.
[10] B.D. Wallace, H. Wang, K.T. Lane, J.E. Scott, J. Orans, J.S. Koo, M. Venkatesh, C. Jobin, L.A. Yeh, S. Mani, M.R. Redinbo, Alleviating cancer drug toxicity by inhibiting a bacterial enzyme, Science 330 (2010) 831–835.
[11] P.M. Gillett, R.A. Schreiber, G.P. Jevon, D.M. Israel, T. Warshawski, H. Vallance, L.A. Clarke, Mucopolysaccharidosis type VII (Sly syndrome) presenting as neonatal cholestasis with hepatosplenomegaly, J. Pediatr. Gastroenterol. Nutr. 33 (2001) 216–220.
[12] S.J. Pellock, B.C. Creekmore, W.G. Walton, N. Mehta, K.A. Biernat, A.P. Cesmat, Y. Ariyarathna, Z.D. Dunn, B. Li, J. Jin, L.I. James, Gut microbial β-glucuronidase inhibition via catalytic cycle interception, ACS Cent. Sci. 4 (2018) 868–879.
[13] B.D. Wallace, et al., Structure and inhibition of microbiome β-glucuronidases essential to the alleviation of cancer drug toxicity, Chem. Biol. 22 (2015) 1238–1249.
[14] D.H. Kim, S.B. Shim, N.J. Kim, I.S. Jang, β-Glucuronidase inhibitory activity and hepatoprotective effect of *Ganoderma lucidum*, Biol. Pharm. Bull. 22 (1999) 162–164.
[15] S. Karak, G. Nag, B. De, Metabolic profile and β-glucuronidase inhibitory property of three species of *Swertia*, Rev. Bras. Farmacogn. 27 (2017) 105–111.
[16] S.Y. Han, C.S. Huh, Y.T. Ahn, K.S. Lim, Y.J. Baek, D.H. Kim, Hepatoprotective effect of lactic acid bacteria, inhibitors of β-glucuronidase production against intestinal microflora, Arch Pharm. Res. (Seoul) 28 (2005) 325–329.
[17] N. Ley, R.J. Bowers, S. Wolfe, Indoxyl-β-D-glucuronide, a novel chromogenic reagent for the specific detection and enumeration of *Escherichia coli* in environmental samples, Can. J. Microbiol. 34 (1988) 690–693.
[18] M.R. Adams, S.M. Grubb, A. Hamer, M.N. Clifford, Colorimetric enumeration of *Escherichia coli* based on β-glucuronidase activity, Appl. Environ. Microbiol. 56 (1990) 2021–2024.
[19] J.R. Haines, T.C. Covert, C.C. Rankin, Evaluation of indoxyl-β-D-glucuronide as a chromogen in media specific for *Escherichia coli*, Appl. Environ. Microbiol. 59 (1993) 2758–2759.
[20] L.J. Moberg, Fluorogenic assay for rapid detection of *Escherichia coli* in food, Appl. Environ. Microbiol. 50 (1985) 1383–1387.
[21] D. Kim, Y. Jin, J. Park, K. Kobashi, Silymarin and its components are inhibitors of β-glucuronidase, Biol. Pharm. Bull. 17 (1994) 443–445.
[22] C.S. Joshi, E.P. Sanmuga, β-Glucuronidase inhibitory effect of phenolic constituents from *Phyllanthus amarus*, Pharm. Biol. 45 (2007) 363–365.
[23] C.A. Simões-Pires, B. Hmicha, A. Marston, K.A. Hostettmann, TLC bioautographic method for the detection of α- and β-glucosidase inhibitors in plant extracts, Phytochem. Anal. 20 (2009) 511–515.
[24] S. Bräm, E. Wolfram, Recent advances in effect-directed enzyme assays based on thin layer chromatography, Phytochem. Anal. 28 (2017) 74–86.
[25] J. Tang, J. Zhou, Q. Tang, T. Wu, Z. Cheng, A new TLC bioautographic assay for qualitative and quantitative estimation of lipase inhibitors, Phytochem. Anal. 27 (2016) 5–12.
[26] E. Azadniya, G.E. Morlock, Automated piezoelectric spraying of biological and enzymatic assays for effect-directed analysis of planar chromatograms, J. Chromatogr. A 1602 (2019) 458–466.
[27] G. Morlock, Chromatography combined with bioassays and other hyphenations – the direct link to the compound indicating the effect, ACS Symp. Ser. 1185 (2014) 101–121.
[28] G. Morlock, W. Schwack, Hyphenations in planar chromatography, J. Chromatogr. A 1217 (2010) 6600–6609.
[29] E. Mahran, I. El Gamal, M. Keusgen, G.E. Morlock, Effect-directed analysis by high-performance thin-layer chromatography for bioactive metabolites tracking in *Primula veris* flower and *Primula boveana* leaf extracts, J. Chromatogr. A 1605 (2019) 460371.
[30] A.M. El-Halawany, M.H. Chung, N. Nakamura, C.M. Ma, T. Nishihara, M. Hattori, Estrogenic and anti-estrogenic activities of *Cassia tora* phenolic constituents, Chem. Pharm. Bull. 55 (2007) 1476–1482.
[31] V. Glavnik, I. Vovk, A. Albreht, High performance thin-layer chromatography–mass spectrometry of Japanese knotweed flavan-3-ols and proanthocyanidins on silica gel plates, J. Chromatogr. A 1482 (2017) 97–108.
[32] R.A. Jefferson, Assaying chimeric genes in plants: the GUS gene fusion system, Plant Mol. Biol. Rep. 5 (1987) 387–405.
[33] Z.M. Weng, P. Wang, G.B. Ge, Z.R. Dai, D.C. Wu, L.W. Zou, T.Y. Dou, T.Y. Zhang, L. Yang, J. Hou, Structure-activity relationships of flavonoids as natural inhibitors against *E. coli* β-glucuronidase, Food Chem. Toxicol. 109 (2017) 975–983.
[34] C. Sekikawa, H. Kurihara, K. Goto, K. Takahashi, Inhibition of β-glucuronidase by extracts of *Chondria crassicaulis*, Bull. Fish. Sci. Hokkaido Univ. 53 (2002) 27–30.
[35] E.W. Frampton, L. Restaino, N. Blaszko, Evaluation of the β-glucuronidase substrate 5-bromo-4-chloro-3-indolyl-β-D-glucuronide (X-Gluc) in a 24-hour direct plating method for *Escherichia coli*, J. Food Protect. 51 (1988) 402–404.
[36] J. Wu, J.R. Stewart, M.D. Sobsey, C. Cormency, M.B. Fisher, J.K. Bartram, Rapid detection of *Escherichia coli* in water using sample concentration and optimized enzymatic hydrolysis of chromogenic substrates, Curr. Microbiol. 75 (2018) 827–834.
[37] I.A. Ramallo, P. García, R.L.E. Furlan, A reversed-phase compatible thin layer chromatography autography for the detection of acetylcholinesterase inhibitors, J. Separ. Sci. 38 (2015) 3788–3794.
[38] J. Seixas de Melo, A.P. Moura, M.J. Melo, Photophysical and spectroscopic studies of indigo derivatives in their keto and leuco forms, J. Phys. Chem. 108 (2004) 6975–6981.
[39] G. Atanasov, et al., Discovery and resupply of pharmacologically active plant-derived natural products: a review, Biotechnol. Adv. 33 (2015) 1582–1614.
[44] Y. Xie, W. Yang, X. Chen, J. Xiao, Inhibition of flavonoids on acetylcholine esterase: binding and structure activity relationship, Food Funct. 5 (2014) 2582–2589.
[45] G.E. Morlock, Background mass signals in TLC/HPTLC–ESI-MS and practical advices for use of the TLC-MS Interface, J. Liq. Chromatogr. Relat. Technol. 37 (2014) 2892–2914.
[46] I. Yüce, H. Agnaniet, G.E. Morlock, New antidiabetic and free-radical scavenging potential of strictosamide in *Sarcocephalus pobeguinii* ground bark extract via effect-directed analysis, ACS Omega 4 (2019) 5038–5043.
[47] G. Ahmad, P.P. Yadav, R. Maurya, Furanoflavonoid glycosides from *Pongamia pinnata* fruit, Phytochemistry 65 (2004) 921–924.
[48] P.S. Colombo, G. Flamini, G. Rodondi, C. Giuliani, L. Santagostini, G. Fico, Phytochemistry of European *Primula* species, Phytochemistry 143 (2017) 132–144.
[40] M.N. Taha, M.B. Krawinkel, G.E. Morlock, High-performance thin-layer chromatography linked with (bio)assays and mass spectrometry – a suited method for discovery and quantification of bioactive components? Exemplarily shown for turmeric and milk thistle extracts, J. Chromatogr. A 1394 (2015) 137–147.
[41] D. Csupor, A. Csorba, J. Hohmann, Recent advances in the analysis of flavonolignans of *Silybum marianum*, J. Pharmaceut. Biomed. Anal. 130 (2016) 301–317.

[42] M. Jamshidi-Aidji, G.E. Morlock, Bioprofiling of unknown antibiotics in herbal extracts: development of a streamlined direct bioautography using *Bacillus subtilis* linked to mass spectrometry, J. Chromatogr. A 1420 (2015) 110–118.
[43] S. Hage, G.E. Morlock, Bioprofiling of Salicaceae bud extracts through high performance thin layer chromatography hyphenated to biochemical, microbiological and chemical detections, J. Chromatogr. A 1490 (2017) 201–211.
[49] M. Shibano, A.S. Lin, H. Itokawa, K.H. Lee, Separation and characterization of active flavonolignans of *Silybum marianum* by liquid chromatography connected with hybrid ion-trap and time-of-flight mass spectrometry (LC–MS/IT-TOF), J. Nat. Prod. 70 (2007) 1424–1428.
[50] Á. Kuki, B. Biri, L. Nagy, G. Deák, J. Kalmár, A. Mándi, M. Nagy, M. Zsuga, S. Kéki, Collision induced dissociation study of the major components of silymarin, Int. J. Mass Spectrom. 315 (2012) 46–54.
[51] B.J. Brinda, H.J. Zhu, J.S. Markowitz, A sensitive LC–MS/MS assay for the simultaneous analysis of the major active components of silymarin in human plasma, J. Chromatogr. B 902 (2012) 1–9.
[52] Á. Kuki, L. Nagy, G. Deák, M. Nagy, M. Zsuga, S. Kéki, Identification of silymarin constituents: an improved HPLC–MS method, Chromatographia 75 (2012) 175–180.